ELSEVIER

Clinical Biomechanics 16 (2001) 415–423

CLINICAL BIOMECHANICS

www.elsevier.com/locate/clinbiomech

A computer model to simulate patellar biomechanics following total knee replacement: the effects of femoral component alignment

J.H. Heegaard [a,*], P.F. Leyvraz [b], C.B. Hovey [a]

[a] *Biomechanical Engineering Division, Department of Mechanical Engineering, Stanford University, Stanford, CA 94305-4040, USA*
[b] *Hôpital Orthopédique de la Suisse Romande, Lausanne, Switzerland*

Received 27 March 2000; accepted 1 March 2001

Abstract

Objective. The objective of this study is to analyze the biomechanics of the patellar component following total knee replacement. More specifically we investigated the effect of displacing the femoral component of an Insall–Burstein II total knee replacement on the patellar tracking and patello-femoral contact pressures.

Design. We used a validated computer simulation of the knee joint to virtually insert the femoral component with the following four types of placements: (1) no misplacement, (2) 5° of internal rotation, (3) 5° of external rotation and (4) 5° of flexion rotation. The patellar 3D tracking and patello-femoral contact pressures were computed for each femoral component placement as a function of knee flexion angle.

Background. Complications at the patello-femoral joint are the among most frequent following total knee replacement.

Results. Femoral component placement unevenly affected the associated patellar tracking: a 5° internal rotation tilted and rotated the patella laterally by about 5° throughout knee flexion. A 5° external rotation of the femoral component had less effect on patellar tracking. A rotation of 5° in flexion primarily caused patellar rotation (5–10° lateral rotation). Femoral component malalignment had only minor effects on the peak pressure distributions at the patello-femoral interface.

Conclusion. These results suggest that femoral component positioning primarily affects patellar tracking, with a possible threat for patellar subluxation under external rotation of the femoral component.

Relevance

Precise alignment of the prosthetic components is difficult to control during total knee replacement due to the lack of precise anatomical landmarks in the human knee joint. Consequently, the position of each prosthetic component may differ from the ideal one suggested by the manufacturer. Improper alignment of the prosthetic components during total knee replacement may lead to premature implant failure.

Keywords: Total knee replacement; Patellar button; 3D tracking; Contact pressure; Femoral component displacement; Knee biomechanics; Computer modeling

1. Introduction

Most current total knee replacement (TKR) systems include resurfacing of both the tibio-femoral and patello-femoral joints. Resurfacing of the patello-femoral joint has been assumed to relieve pain and provide better knee extension function following TKR [1]. Long-term clinical results have demonstrated however, that the resurfaced patello-femoral joint is the source of many complications (estimated between 5% and 30% [2]) mostly due to tracking instability, surface wear, fractures and loosening [3]. Higher stress and strain levels in the resurfaced patella [4] were found to favor wear and fracture of the plastic button [3].

Previous studies on patellar biomechanics have reported important changes in patellar tracking following TKR [5]. In particular the positioning of the femoral component, which is largely under the surgeon's control at insertion time, has been recognized as an important factor influencing patellar tracking. In some cases, external rotation of the femoral component was found to restore better patellar tracking and improve patellar stability [6].

* Corresponding author.
E-mail address: heegaard@bonechip.stanford.edu (J.H. Heegaard).

0268-0033/01/$ - see front matter
PII: S0268-0033(01)00020-1

In addition to tracking changes, TKR also leads to increased patello-femoral contact pressures during knee flexion [7]. In contrast to the healthy knee, in which conformity between the articulating surfaces is optimal, the patello-femoral contact zones are significantly reduced after TKR due to a loss of congruence between the replaced articular surfaces [8]. These higher contact pressures may also contribute to joint surface deterioration and accelerated wear of the plastic button [9]. Central positioning of the patellar component has been reported to optimally distribute the patello-femoral contact pressure [10]. Similarly restoration of the standard patellar thickness following patellar component insertion minimized possible patello-femoral contact forces [11]. Little is known however, on the possible influence of femoral component alignment on patello-femoral pressure distribution.

The objective of this study was to determine the variations of patellar tracking and patello-femoral contact pressure induced by rotational misplacements of the Insall–Burstein II (IB2) femoral component. The biomechanical variables of interest were computed during knee flexion using a validated 3D computer model [12].

2. Methods

2.1. Mathematical knee model

A validated 3D finite element model of the patello-femoral joint [12] was used to compute the patellar 3D tracking and contact pressure as a function of knee flexion (Fig. 1). The model was also capable to simulate the insertion of the femoral and patellar components in the virtual knee model.

The patella was modeled as a core of cancellous bone surrounded by a shell of cortical bone, covered by a cartilage layer delimitting the articular surface. The anatomy of the joint was obtained from 1 mm thick sagittal CT-scans (Somatron DR3, Siemens, Germany) of a 68 yr old female cadaver knee. The resolution of each scan was 256×256 pixels for a field of view of 14 cm. The 3D mesh of the patella was obtained by assembling the segmented 2D slices. The corresponding mechanical properties were taken from published values (Table 1). The patella was discretized into 950 tri-linear hexahedral elements. The patellar tendon (PT), connecting the patella to the tibial tuberosity, was discretized into three nonlinear string-type elements representing lateral, central and medial fibers whose anatomical insertions were measured using Roentgen stereo-photogrammetry analysis (RSA) [13]. The femoral condyles were modeled as rigid surfaces (16-nodes bicubic Hermite patches.) The shape of these surfaces were measured directly from the specimen bones using stereo-photogrammetric curve reconstructions (SCR) [14] and discretized into a regularly spaced set of 250 points fitting the femoral groove surface.

These finite element models were then coupled to a large scale model of the right leg. We modeled the limb segments (thigh and shank) as rigid bodies. The femur was held fixed during knee flexion, and the tibia was flexed from 0° to 150° in 15° increments. The motion of the tibial insertion points of the PT were therefore known. The successive positions of these points were recorded during a preliminary experiment using RSA

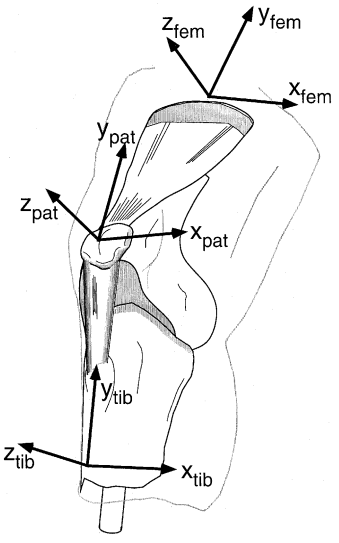

Fig. 1. Reference frames used to specify patellar and tibial tracking with respect to a fixed femur. The three rotations of the patella, (i.e. flexion, tilt and rotation), are defined by the rotations of the patellar frame (x_{pat}, y_{pat}, z_{pat}) with respect to the fixed femoral frame. Translation of the patella with respect to the femur (shift along the x-axis and y–z translation) is defined by the translation of the center of the patella with respect to the femoral frame.

Table 1
Material properties used for the knee model

	λ (MPa)	μ (MPa)	E (MPa)	v
Cortical bone	8.65×10^3	5.76×10^3	1.50×10^4	0.30
Cancellous bone	1.73×10^2	1.15×10^2	3.00×10^2	0.30
Cartilage	1.06×10^1	6.80×10^{-1}	2.00	0.47
UHMWPE	7.14×10^2	1.78×10^2	5.00×10^2	0.40
Patellar tendon	0.00	5.00×10^1	10^2	0.00

[15]. In the computer model, knee flexion angles were only considered between 45° and 135° for stability reasons. A pulling force with a constant magnitude of 40 N, representing the quadriceps action, was equally distributed on three nodes of the patellar base. The direction of these individual forces varied during flexion to account for the wrapping of the muscle bundles around the femoral groove in the sagittal plane and for the effects of the *Q*-angle in the frontal plane. The pulling directions were obtained at each time step from the preliminary measurements of knee kinematics on each specimen. Six radio-opaque markers were inserted on the anterior surface of the rectus femoris and their 3D position measured during knee flexion. Pairs of pellets were then used to define muscle fiber orientation at each flexion step.

The patello-femoral joint interface was modeled by a set of 100 large slip contact elements [16,17]. Contact was assumed frictionless based on the low coefficient of friction typically reported for lubricated synovial joints [18]. The contact interaction is governed by the principle of action and reaction which takes the following discrete local form:

$$\boldsymbol{p} = \boldsymbol{p}^{c} = -\boldsymbol{p}^{1}, \tag{1}$$

where $\boldsymbol{p}$ is the contact force exerted by a striker node $\boldsymbol{y}^1$ on the rigid obstacle at $\boldsymbol{y}^c$, and $\boldsymbol{p}^1$ is the reaction at $\boldsymbol{y}^1$. This force is distributed on the striker node according to the discrete principle of virtual work. More specifically

$$\delta W_c = \boldsymbol{p}(\boldsymbol{g}(\boldsymbol{u})) \cdot \delta \boldsymbol{g}(\boldsymbol{u}) = \boldsymbol{f}(\boldsymbol{u}) \cdot \delta \boldsymbol{u} = \delta W, \tag{2}$$

i.e., the virtual work δW_c developed by the contact force $\boldsymbol{p}(\boldsymbol{g}(\boldsymbol{u}))$ through a variation of the contact distance $\boldsymbol{g}(\boldsymbol{u})$ must be equal to the virtual work δW developed by the element nodal force $\boldsymbol{f}^1$ through the corresponding nodal displacements variation $\delta \boldsymbol{u}$. In the frictionless case, the contact force is directed along the target facet normal $\hat{\boldsymbol{n}}$ and is written as

$$\boldsymbol{p} = f_n \hat{\boldsymbol{n}}. \tag{3}$$

The gap distance $g_n = \boldsymbol{g} \cdot \hat{\boldsymbol{n}}$ is related to the conjugate pressure f_n by a (multivalued non-differentiable) unilateral contact law. At the interface, the frictionless contact law is locally characterized by three complementary Signorini conditions

$$g_n \geqslant 0, \quad f_n \leqslant 0, \quad g_n f_n = 0, \tag{4}$$

respectively, expressing that the contacting bodies cannot penetrate each other, cannot pull on each other and are either separated or pressing on each other.

All the applied forces being assumed conservative, equations of motion can be obtained by minimizing the total energy $\pi(\boldsymbol{u})$ defined as the difference between the internal elastic strain energy $\phi(\boldsymbol{u})$ stored in the patella and the potential energy $\eta(\boldsymbol{u})$ of the applied forces

$$\pi(\boldsymbol{u}) = \phi(\boldsymbol{u}) - \eta(\boldsymbol{u}). \tag{5}$$

By including the first Signorini condition to this last equation, the problem reduces to find a constrained local minimum of $\pi(\boldsymbol{u})$

$$\begin{array}{ll} \min_{\boldsymbol{u}} & \pi(\boldsymbol{u}) := \phi(\boldsymbol{u}) - \eta(\boldsymbol{u}), \\ \text{s.t.} & \boldsymbol{g}_n(\boldsymbol{u}) \in \boldsymbol{R}^M_+, \end{array} \tag{6}$$

where $\boldsymbol{g}_n(\boldsymbol{u})$ represents an M-dimensional vector, whose components contain the gap distances of the M contact elements used to discretize the interface between the contacting bodies.

The resulting inequality constrained minimization problem is then transformed into an unconstrained saddle point problem using augmented Lagrangian multipliers.

Using a mixed form extension of the above variational principle [19], the corresponding augmented Lagrangian contact force operator $\boldsymbol{p} \in \boldsymbol{R}^3$ expresses as [16]:

$$\boldsymbol{p} = \begin{cases} \begin{pmatrix} -(f_n + r g_n)\hat{\boldsymbol{n}} \\ g_n c \end{pmatrix} & \text{if } (f_n + r g_n) \leqslant 0 \quad \text{(contact)} \\ \begin{pmatrix} \boldsymbol{0} \\ -f_n / r \end{pmatrix} & \text{if } (f_n + r g_n) > 0 \quad \text{(gap)}, \end{cases} \tag{7}$$

where r is a regularization parameter, and f_n is the Lagrange multiplier holding the unknown contact force magnitude.

A detailed description of the method can be found in [16]. The main features of this method are to lead to well-conditioned contact problems in contrast to penalty methods. The resulting finite element problem was solved using the program TACT [20].

2.2. Total knee replacement simulation

A medium size (A/P 65 mm) femoral component of an IB2 Total Condylar prosthesis (Zimmer, Warsaw, IN, USA) was digitized with an accuracy of 10 μm, into 2000 points (25 slices of 80 points) using a custom made digitizer [21]. The digitized components were then inserted into the finite element model of the knee. For simulation purposes, three criteria were considered for defining the digitized femoral component standard position (Fig. 2(a)):

1. In the sagittal plane, the central part of the flange was aligned along the diaphyseal axis.
2. In the frontal plane, the prosthesis was oriented with a 6° valgus angle between the groove and the femoral diaphyseal axis.
3. In the transverse plane, the implant was aligned along the axis defined by the most anterior points on the lateral and medial condyles.

The patellar cartilage layer and the underlying cortical shell were removed and a medium sized patellar button (34 mm of diameter), with a spherical dome shape, was inserted so as to preserve the original patellar thickness

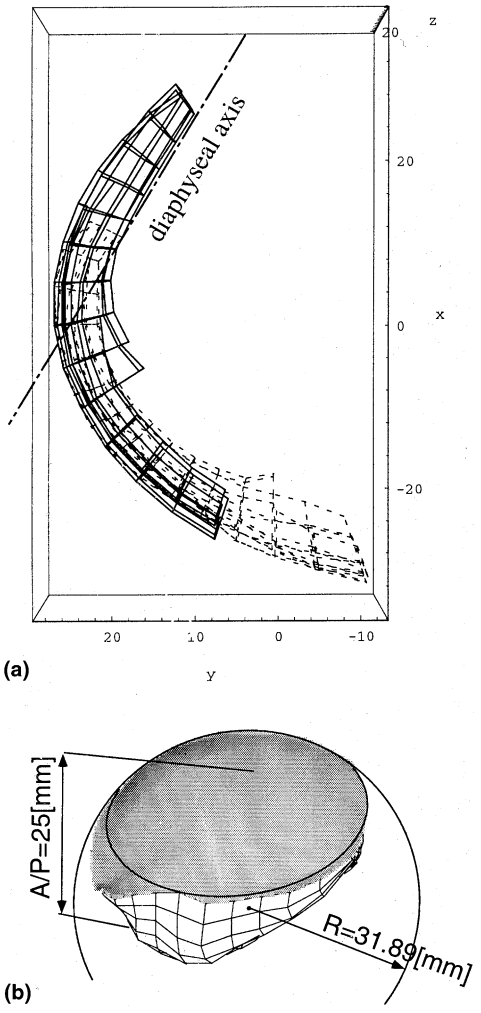

Fig. 2. (a) Sagittal view of the Total Condylar femoral component insertion. Dashed lines represent the natural knee surface and solid lines the femoral component. (b) Patellar button insertion procedure to preserve original patellar thickness.

[22]. This procedure was simulated by positioning a spherical cap with a radius of 31.89 mm corresponding to the patellar button radius of curvature (Fig. 2(b)). The 3D tracking of the patella and the contact pressure on the patellar button as a function of knee flexion was then computed for this standard placement of the femoral component.

Finally, insertion of the femoral component into the model was simulated with three non-standard placements, corresponding to a 5° external, internal or flexion rotation. These displacements were obtained by rotating the component's surface around the appropriate axis and by translating the rotated surface so as to keep a correct femoral groove depth. The resulting patellar tracking and pressure distributions were computed for each case as a function of knee flexion.

The 3D tracking of the patella was defined in terms of its flexion (rotation about the femoral x-axis – see Fig. 1 for axes definition), tilt (rotation about femoral y-axis), rotation (rotation about the femoral z-axis), shift (translation along the femoral x-axis) and translations along the femoral y and z axes [16]. Intact knee kinematics referred to those computed before replacing the articular surfaces with the prosthetic components. Negative tilt angles indicate a lateral tilt. Negative rotation angles indicate a lateral rotation of the patella (i.e., counter-clockwise around the femoral z-axis). Finally, a negative shifts indicates a lateral translation of the patella along the femoral x-axis.

3. Results

3.1. Standard knee arthroplasty

When compared to intact knee kinematics, the patellar tracking parameters most affected by TKR were tilt (Fig. 3(b)), which increased by about 8° throughout knee flexion, and rotation (Fig. 3(c)), which increased similarly by about 5°. The slope of the medio-lateral shift (Fig. 3(d)) was slightly steeper, indicating a quicker rate of lateral shift than in the intact knee. The other tracking parameters including flexion (Fig. 3(a)), shift (Fig. 3(d)) and sagittal translation (Figs. 3(e) and (f)) did not change markedly after TKR.

The contact patterns, which for the intact knee patella evolved from the distal apex to the proximal pole during progressive flexion, extended over significantly smaller areas after TKR. The medial contact zone shifted toward the medial edge of the patellar button. The range of distal-proximal contact zone displacement during flexion was reduced, but could still be characterized by a proximal shift up to 90° of knee flexion, followed by a distal shift at higher degrees of flexion (Fig. 4). Pressure gradients were higher, as shown by the closer succession of contact pressure contour lines.

The peak pressures were higher on the lateral compartment than on the medial one (Fig. 5). After TKR most of the pressure was distributed on the lateral side, with an average 0.5 MPa increase in the peak pressures.

3.2. Internal misplacement

A 5° internal rotation of the femoral component produced noticeable changes on the patellar tracking. The patella tilted laterally by about 5° throughout knee flexion (Fig. 3(b)), and rotated laterally by a comparable amount (Fig. 3(c)). The internal rotation of the femoral component also resulted in a medial shift of the patella by about 4 mm (Fig. 3(d)). The other tracking parameters were not noticeably affected by this femoral component misplacement. Internal rotation of the femoral component also produced patellar tracking closer to that of the intact knee, especially for patellar tilt and rotation (Figs. 3(b) and (c)).

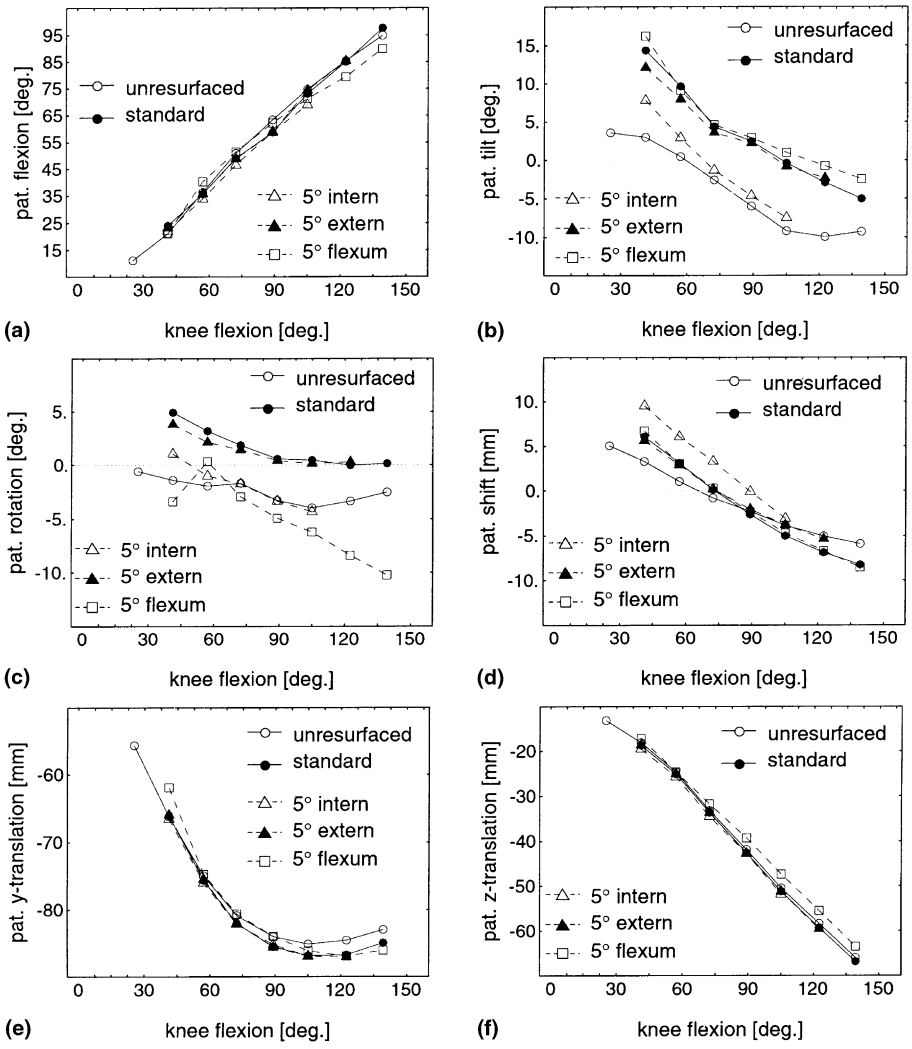

Fig. 3. Patellar 3D tracking of knee 1 as a function of knee flexion, for the natural knee, after standard TKR and for three types of femoral component misplacements: 5° internal or external rotation and 5° flexion.

The patellar contact areas shifted laterally on both facets (Fig. 6) as they shifted proximally during mid-flexion angles and then shifted backward distally during the last phase of knee flexion.

Internal rotation of the femoral component produced a small overall increase of peak pressure which was more marked on the medial compartments (+0.15 MPa) than on the lateral one (+0.05 MPa) (Fig. 7).

3.3. External misplacement

A 5° external rotation of the femoral component, unlike internal rotation misplacement, did not affect the patellar tracking in a significant way. Differences between the tracking parameters for the standard positioned and externally rotated femoral component were below 1° for the rotations and below 2 mm for the translations.

Similarly, contact patterns were not affected by external rotation of the femoral component, and could not be distinguished from those computed in the standard position case (Fig. 6).

The mean peak pressure was only slightly increased on the medial compartment (+0.03 MPa) and slightly decreased on the lateral one (−0.04 MPa) (Fig. 7).

3.4. Flexion misplacement

When the femoral component was inserted with a 5° flexion rotation, patellar rotation was primarily affected, with an additional external rotation reaching almost 10° at 105° of knee flexion. This represented the largest deviation observed among all the femoral component displacements (Fig. 3(c)). Patellar flexion also decreased at higher knee flexion angles (Fig. 3(a)), but to a lesser extent.

Similarly to the external rotation of the femoral component, the flexion rotation did not change the patellar contact patterns during knee flexion (Fig. 6). However, flexion displacement produced a small in-

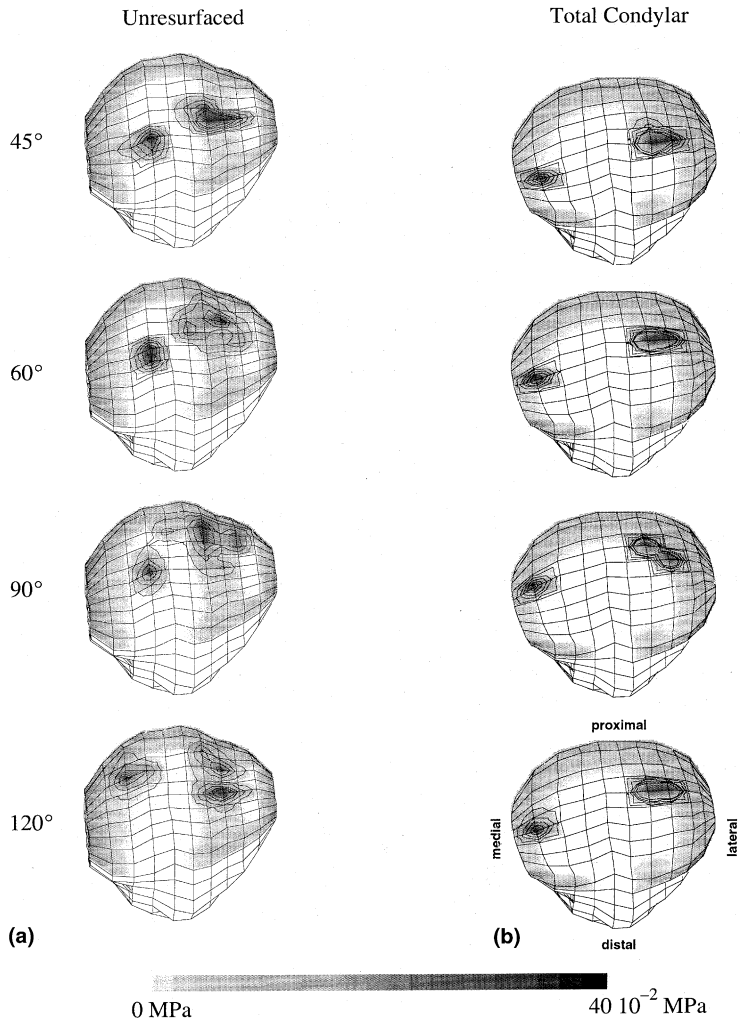

Fig. 4. Patello-femoral contact pressures for knee specimen 1 at 45°, 60°, 90° and 120° of knee flexion, before (a) and after standard TKR (b).

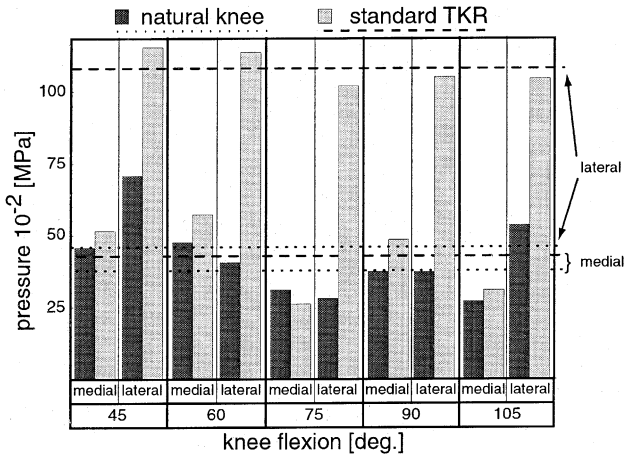

Fig. 5. Peak pressures on the medial and lateral contact surface as a function of knee flexion, before (black) and after standard TKR (light gray).

crease of the average pressure by 0.05 MPa on the medial facet and by 0.08 MPa on the lateral one. No consistent pressure increase could however be seen at individual flexion angles on either facets.

4. Discussion

Many factors have been attributed to cause patellar dislocation after TKR. Incorrect positioning of any of the components of the prosthesis, inadequate lateral release, and failure of medial structures repair have been recognized as factors favoring patellar subluxation [23,24]. Although these factors have been extensively discussed in the clinical literature, only a few biomechanical studies have been conducted to quantitatively evaluate their effects on patellar tracking [6,25,26]. In particular, positioning of the femoral component has recently been recognized as an important factor influencing patellar tracking after TKR [5,26]. It must be

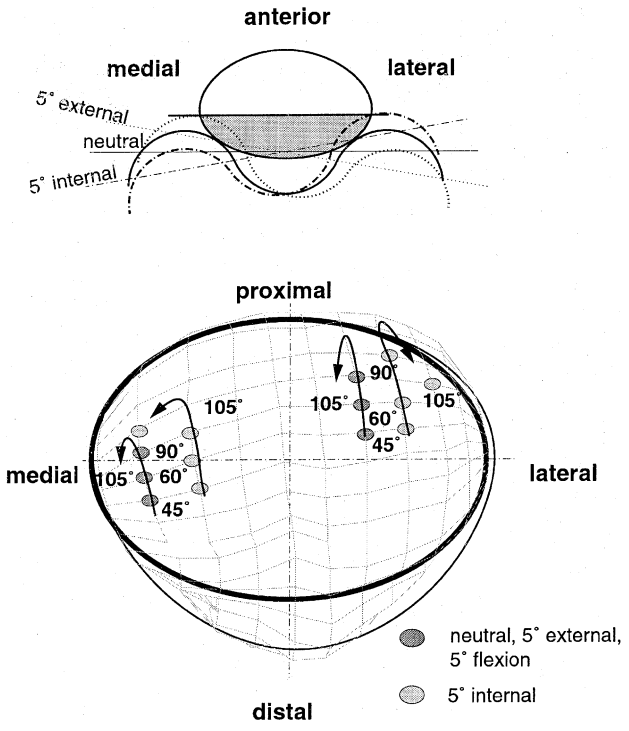

Fig. 6. Motion of the centers of contact areas during knee flexion for the standard TKR and for the three displacements (5° internal, external and flexion rotation).

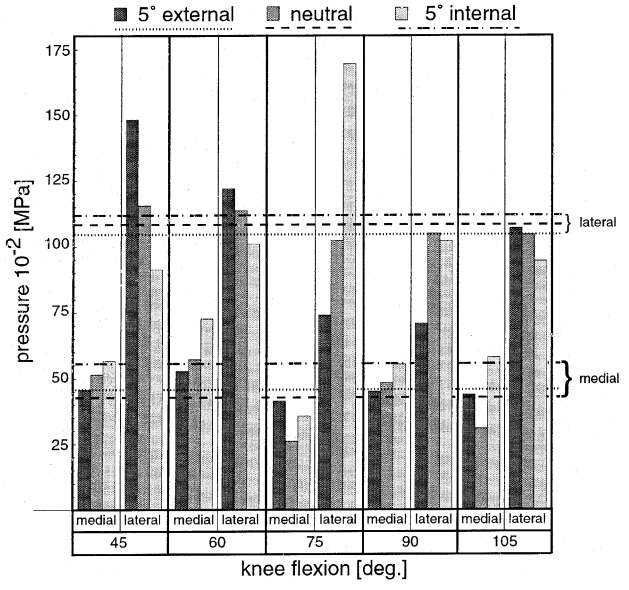

Fig. 7. Peak pressures on the medial and lateral contact surface as a function of knee flexion, for standard TKR and with a 5° external or internal rotation of the femoral component.

noted however, that these studies did not elucidate the possible role of femoral component positioning on patellar pressure distribution. It has been hypothesized that variations in patellar tracking cause excessive patellar wear due to shear force increases at the joint interface [9]. More specifically, excessive medial displacement of the patella and increase in Q-angle appeared to be the main factors affecting patellar failure in TKR.

In the present study, patellar tracking and pressure distribution was computed after a TKR using the IB2 prosthesis. Variations of tracking and pressure patterns were induced by inserting the femoral component with 5° internal or external rotation, or with a 5° flexion rotation. The amount of rotational misplacement was chosen to reflect a reasonable maximum amount of uncertainty encountered during surgery.

The most sensitive parameters to femoral component displacement were patellar tilt and rotation, as could be observed from comparisons between patellar tracking curves for the standard insertion and following rotation displacement (Figs. 3(b)–(d)). This was especially noticeable after internal rotation of the femoral component. This rotation also shifted the patella medially by almost 5 mm throughout the considered flexion range. These trends compared well with those previously reported by Rhoad et al. [6]. They reported an additional medial shift ranging from 4 to 7 mm during knee flexion using an AMK femoral component (Depuy, Warsaw, IN, USA) inserted with a 10° internal rotation. Inserting the femoral component with internal rotation resulted in a patellar tracking which was overall closer to the one of the natural knee (Figs. 3(b) and (c)). The external flange of the component then became more prominent than the internal one, hence tilting and rotating the patella laterally.

On the other hand, external rotation of the IB2 femoral component did not affect patellar tracking. Previous studies [5,26] have reported however, that external rotation of the femoral component restored patellar tracking closer to that occurring in the intact knee. It must be noted that the femoral component of the IB II used in the present study, unlike the AMK one, does not constrain the patella medially with a higher lateral ridge, but consists instead of a symmetric toroidal groove. In view of the present results, the constraints controlling the I-B II patellar button motion were hardly affected by moderate external rotations (i.e, not exceeding 5°).

Inserting the femoral component with 5° of flexion primarily produced an additional 5° lateral patellar rotation (Fig. 3(c)) throughout knee flexion. This type of malalignment, although never studied before, is however believed to potentially occur in surgical practice, due to the short length of the trochlear area used for flexion–extension alignment of the femoral component. Similarly to external femoral rotation, flexion rotation of the femoral component did not modify patellar tracking. This could again be imparted to the symmetry of the femoral groove in the sagittal plane.

The sagittal motion of the patella, described by its flexion and y–z translation was hardly affected by TKR

and by femoral component malalignment (Figs. 3(a), (e) and (f)) reflecting the close fit between the femoral component and the anatomical femur sagittal shapes.

The smaller range of contact zone motion observed during knee flexion after TKR compared well with a previous study by Hassenpflug [7], who experimentally reported a maximal path of 9 mm for the contact points on the IB2 patellar button. In their previous study, Rhoads et al. [6] hypothesized that variations of patellar tracking following femoral component displacement would also affect contact pressure at the patello-femoral interface. The high lateral ridge of the AMK femoral component and internal rotation or medial displacement of this component was assumed to produce unacceptable increase of contact pressure. In the present model however, no noticeable contact pressure increase occured. Rotation displacements of the femoral component produced only small variations in the peak contact pressure on the medial compartment of the patellar button.

The patellar contact areas moved laterally after internal rotation of the femoral component. At the same time the patella tilted and shifted laterally indicating a lateral sliding of the patella with respect to the femoral component (as opposed to lateral rolling). Similar observations were already reported in earlier patellar tracking studies following TKR [5,6]. In the present study, additional insight was gained on the contact patterns distribution.

Fatigue wear of the patellar button is among the most commonly observed problems with incongruent prosthetic designs [27,28]. Buechel et al. [29] have evaluated contact stresses in patellar button of six commonly available designs, including the IB2, under physiological loads. The peak contact stresses for this prosthesis was higher than the 5 MPa maximum level recommended by polyethylene manufacturers. In the present simulations the same loads were applied on the quadriceps (40 N) as those applied during an earlier experiment [16]. The resulting peak contact pressure were about 1 MPa, much lower values than the 5 MPa limit. However, when physiological loads would be applied, the contact pressure would increase following a quadratic relation according to Hertzian contact theory. Physiological quadriceps load typically range between 2 and 3 times body weight, so that the currently applied load of 40 N load would only represent about 1/15 body weight. Under normal physiological loading, the contact pressure would thus become in the order of magnitude of 10 MPa.

To summarize, modifying the insertion position of the femoral component of the IB2 prosthesis did affect patellar biomechanics. Rotating the femoral component 5° internally produced a patellar kinematics closer to the one of the natural knee with no marked increase of contact pressure. A 5° external rotation of the femoral component had less incidence on patellar tracking, which could indicate some tolerance during insertion with respect to this parameter. None of the applied displacement noticeably altered the contact pressure. Therefore, stability of the patella should be of primary concern to the surgeon, as patellar tracking was affected by positioning of the femoral component. On the other hand, pressure distribution depended mainly on the femoral components geometry as it was not noticeably affected by femoral components displacement.

Acknowledgements

This work was supported by grants from the Swiss National Fund (to JHH & PFL), the Department of Veterans Affairs and the National Science Foundation (to CBH).

References

[1] Rand JA. Current concepts review the patellofemoral joint in total knee arthroplasty. J Bone Joint Surg 1994;76-A:612–20.
[2] Merkow RL, Soudry M, Insall JN. Patellar dislocation following knee replacement. J Bone Joint Surg 1985;67-A:1321.
[3] Windsor RE, Scuderi GR, Insall JN. Patellar fractures in total knee arthroplasty. J Arthroplasty 1989;4(Suppl):63–7.
[4] McLain RE, Bargar WF. The effect of total knee design on patellar strain. J Arthroplasty 1986;1:91–8.
[5] Anouchi YS, Whiteside LA, Kaiser AD, Milliano MT. The effects of axial rotational alignment of the femoral component on knee stability and patellar tracking in total knee arthroplasty demonstrated on autopsy specimens. Clin Orthop 1993;287:170–7.
[6] Rhoads DD, Noble PC, Reuben JD, Mahoney OM, Tullos HS. The effect of femoral component position on patellar tracking after total knee arthroplasty. Clin Orthop 1990;260:43–51.
[7] Hassenpflug J. Das Patellofemoralgelenk beim kuenstlichen Kniegelenkersatz. Berlin: Springer; 1989.
[8] Benjamin JB, Szivek JA, Hammond AS, Kubchandhani Z, Matthews AI, Anderson P. Contact areas and pressures between native patellas and prosthetic femoral components. J Arthroplasty 1998;13:693–8.
[9] Hsu HP, Walker PS. Wear and deformation of patellar components in total knee arthroplasties. Clin Orthop 1989;246:260–5.
[10] Lee TQ, Budoff JE, Glaser FE. Patellar component positioning in total knee arthroplasty. Clin Orthop Rel Res 1999;366:274–81.
[11] Hsu HC, Luo ZP, Rand JA, An KN. Influence of patellar thickness on patellar tracking and patellofemoral contact characteristics after total knee arthroplasty. J Arthroplasty 1996; 11:69–80.
[12] Heegaard JH, Leyvraz PF, Curnier A, Rakotomanana L, Huiskes R. Biomechanics of the human patella during passive knee flexion. J Biomech 1995;28:1265–79.
[13] Huiskes R, Kremers J, De Lange A, Woltring HJ, Selvik G, van Rens TJ. Analytical stereophotogrammetric determination of three-dimensional knee-joint geometry. J Biomech 1985;18:559–70.
[14] Meijer RC, Huiskes R, Kauer JM. A stereophotogrammetric method for measurements of ligament structure. J Biomech 1989;22:177–84.

[15] Heegaard JH, Leyvraz PF, van Kampen A, Rakotomanana L, Rubin PJ, Blankevoort L. Influence of soft structures on patellar 3D tracking. Clin Orthop Rel Res 1994;299:235–43.
[16] Heegaard JH, Curnier A. An augmented Lagrangian method for discrete large slip contact problems. Int J Numer Meth Eng 1993;36:569–93.
[17] Heegaard JH, Curnier A. Geometric properties of 2D and 3D unilateral large slip contact operators. Comput Meth Appl Mech Eng 1996;131:263–86.
[18] Mow VC, Soslowsky LJ. Friction, lubrication, and wear of diarthrodial joints. In: Mow VC, Hayes WC, editors. Basics orthopaedic biomechanics. New York: Raven Press; 1991. p. 245–92.
[19] Alart P, Curnier A. A mixed formulation for frictional contact problems prone to Newton like methods. Comput Meth Appl Mech Eng 1991;9:353–75.
[20] Curnier A. TACT: a contact analysis program. In: Maceri F, DelPiero G, editors. Unilateral problems in structural analysis – 2, CISM 304. Wien: Springer; 1985. p. 97–116.
[21] Essinger J, Leyvraz PF, Heegaard JH, Robertson DD. A mathematical model for the evaluation of the behaviour during flexion of condylar type knee prostheses. J Biomech 1989;22: 1229–41.
[22] Reuben JD, McDonald CL, Woodard PL, Hennington LJ. Effect of patella thickness on patella strain following total knee arthroplasty. J Arthroplasty 1991;6:251–8.
[23] Briart JL, Hungerford DS. Patellofemoral instability in total knee arthroplasty. J Arthroplasty 1989;4(Suppl):87–93.
[24] Mochizuki RM, Shurman DJ. Patellar complications following total knee arthroplasty. J Bone Joint Surg 1979;61-A:879.
[25] Kaltwasser P, Uematsu O, Walker PS. The patellofemoral joint in total knee replacement. In: Proceedings of the 33rd Annual Meeting, ORS; 1987. p. 292.
[26] Rhoads DD, Noble PC, Reuben JD, Tullos HS. The effect of femoral component position on the kinematics of total knee arthroplasty. Clin Orthop 1993;286:122–9.
[27] Cameron HU, Hunter GA. Failure in total knee arthroplasty: mechanisms, revisions and results. Clin Orthop 1982;170:141–9.
[28] Stulberg SD, Stulberg BN, Mamati Y, Tsao A. Failure mechanisms of metal-backed patellar components. Clin Orthop 1988;236:88–105.
[29] Buechel FF, Pappas MJ, Makris G. Evaluation of contact stress in metalbacked patellar replacement. Clin Orthop 1991;273: 190–7.